

## The strontium and oxygen isotopic record of hydrothermal alteration of syenites from the Abu Khruq complex, Egypt

Timothy M. Lutz<sup>1</sup>, Kenneth A. Foland<sup>1,\*</sup>, Henry Faul<sup>1,†</sup>, and LeeAnn Srogi<sup>1,\*\*</sup>

<sup>1</sup> Department of Geology, University of Pennsylvania, Philadelphia, PA 19104, USA

**Abstract.** Hydrothermal convection initiated by emplacement of the gabbro-syenite complex of Abu Khruq into the Egyptian basement 89 Ma ago systematically altered the trace element and isotopic compositions of the syenites. The scale of Sr transport in migrating solutions was far larger than the scale of Sr isotopic equilibration within rocks. As a result, Sr exchange was heterogeneous in the syenites, an effect which can be observed on three different scales. Within grains of a single mineral species, heterogeneities are related to grain boundaries and microfractures through which fluids migrated. Among minerals within rock samples, heterogeneities are related to differences in susceptibility to Sr alteration. Among samples within a single unit, heterogeneous alteration is apparently related to differences in permeability close to fracture zones.

During the early stages of alteration radiogenic Sr derived from the country rocks was added to the syenites, causing small net changes in concentration (5 ppm ave.). Some Rb–Sr mineral isochrons from single rock samples yield the emplacement age because isotopic equilibration of this added Sr sometimes occurred within rock specimens. However, regressions of the whole-rock Rb–Sr data yield apparent ages that are about 10 Ma too old. Later stage alteration involved larger changes in whole-rock Sr concentration (45 ppm ave.) but had little further effect on the isotopic relationships because the Sr was derived from co-genetic gabbros rather than the country rocks.

Alterations of Rb, Sr, and Sr isotopic compositions are not well correlated with changes in  $^{18}\text{O}/^{16}\text{O}$  ratio because mineralogy played an important role in decoupling trace element and oxygen isotopic alteration. In general, the absence of such correlations for whole-rock data is not diagnostic of rocks with unaltered trace element and isotopic compositions. Mineral-scale Sr isotopic heterogeneities associated with grain boundaries and microfractures may be the most unambiguous evidence of trace element mobility.

lating meteoric waters is common. Modifications of the trace element and isotopic compositions of basaltic and ophiolitic rocks during hydrothermal exchange have been amply documented (McCulloch et al. 1981; Dickin and Jones 1983; Spooner et al. 1977). Taylor (1977, 1978) has shown that hydrothermal interaction with epizonal granites may have profound effects on oxygen and hydrogen isotopes. Other studies of granitic rocks have examined the effects of hydrothermal alteration and assimilation/fractional crystallization on trace element and isotopic compositions (Stuckless et al. 1981; Schleicher et al. 1983; Fleck and Criss 1985; Johnston and Black 1986; Cathelineau 1987; Criss and Fleck 1987).

In some rocks which show pervasive hydrothermal alteration of oxygen isotope ratios, there are no correlations of  $\delta^{18}\text{O}$  with trace element contents or isotopic compositions (e.g.,  $^{87}\text{Sr}/^{86}\text{Sr}$  ratios). This lack of correlation sometimes is taken to indicate the absence of pervasive, systematic alteration of rock chemistry (Perfit et al. 1980; Walsh et al. 1979). Walsh et al. (1979, p. 99) found that “correlations of  $\delta^{18}\text{O}$  with other major and trace element data and  $^{87}\text{Sr}/^{86}\text{Sr}$  ratios are uniformly low ... thus it is unlikely that the interaction of the rocks with meteoric water has systematically altered the chemical (including Sr isotopic) characteristics” of granites at the Isle of Mull.

The absence of a correlation between O isotopic and trace element chemistry in whole-rock samples does not rule out hydrothermal alteration on a smaller scale within samples. For example, Dickin (1983) and Dickin et al. (1980) have reported modification of Sr isotopic compositions in samples associated with fractures in granites. Apparently, hydrothermal fluid migration through permeable zones facilitates trace element mobility in the rocks near them. Cathelineau (1987) showed that trace element mobility during hydrothermal alteration may be controlled by subsolidus mineral reactions and anionic complexing in the fluid.

This paper presents data from the Abu Khruq complex in Egypt that indicate that the Sr content and Sr isotopic composition of alkali syenites were significantly modified by hydrothermal exchange without producing obvious correlations with  $\delta^{18}\text{O}$ . Significant changes in whole-rock trace element concentrations occurred via the alteration of volumetrically small portions of mineral grains by reaction and the development of diffusion rims or adsorption zones along grain boundaries and microfractures. The effects of hydrothermal alteration were controlled both by variations in the permeability and differential susceptibilities of miner-

### Introduction

Studies of the  $^{18}\text{O}/^{16}\text{O}$  and D/H ratios of igneous rocks have demonstrated that hydrothermal alteration by circu-

\* *New address:* Department of Geology and Mineralogy, Ohio State University, Columbus, OH 43210, USA

\*\* *New address:* Department of Geology, Smith College, Northampton, MA 01063, USA

† Deceased on 9/81

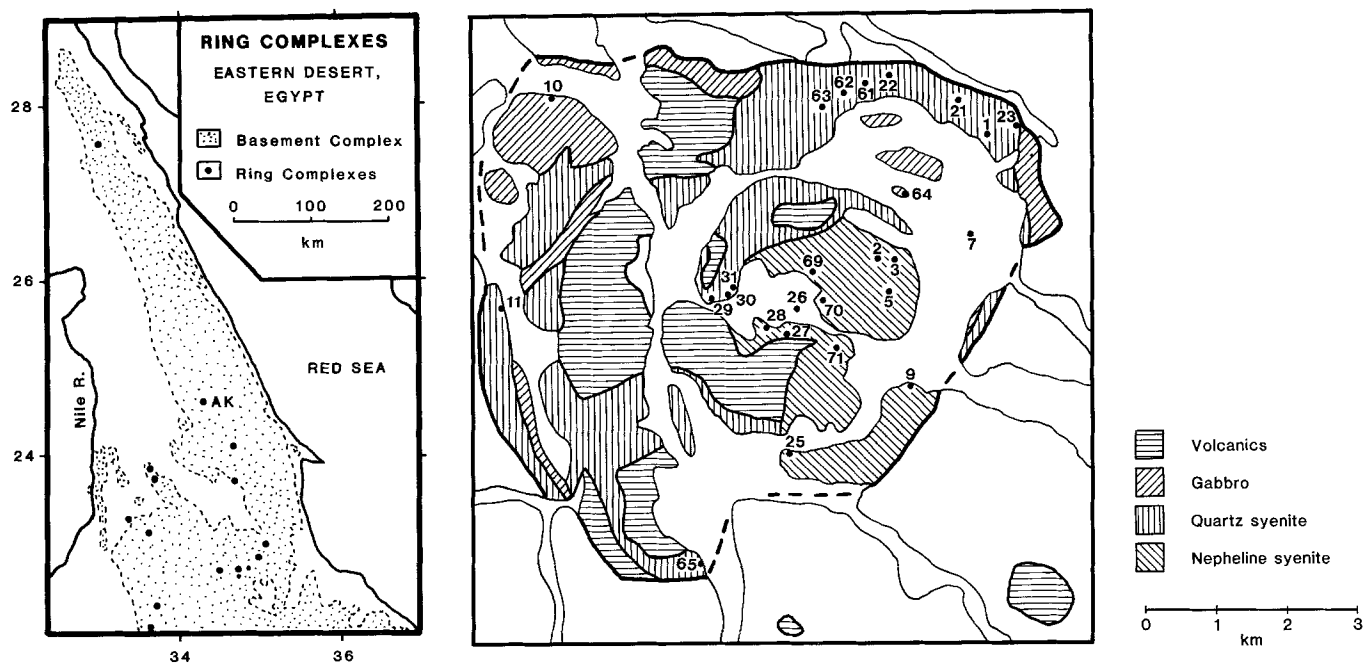


Fig. 1. Geologic map of the Abu Khruq complex simplified from El Ramly et al. (1971). Unpatterned areas represent wadis (within the complex) or basement rocks (outside the complex)

als to reaction and alteration. The most significant result is that the role of hydrothermal processes in governing trace element and isotopic compositions cannot, in general, be deduced from measurements made on whole-rock samples without regard to their mineralogy.

### Geology of the Abu Khruq complex

The Abu Khruq complex is located in the Eastern Desert of Egypt, roughly midway between the Nile River and the Red Sea. It is a member of an alkaline province including complexes of similar size, structure, and composition which crop out along the western margin of the Red Sea in Egypt, Sudan, Ethiopia, and Libya (Nearry et al. 1976; Vail 1976). These rocks represent episodic alkaline magmatism which continued from the Cambrian to the Cretaceous (Serencsits et al. 1981). Within the basement of the Eastern Desert of Egypt there are at least fourteen major centers of associated plutonic and volcanic activity and many smaller centers (El Ramly et al. 1969a, b, 1971, 1979; El Ramly and Hussein 1985). The Egyptian complexes typically consist of early undersaturated gabbroic rocks of alkaline affinity, oversaturated and/or undersaturated syenites, and alkaline trachytes or rhyolites. Chemical analyses (El Ramly et al. 1969a, b, 1971) suggest a composition gap between gabbroic and syenitic rocks at all complexes.

Abu Khruq is a ring complex about 7 km across emplaced into the Proterozoic basement about 85 km from the Red Sea (Fig. 1). The geology of the central portion of the complex has been mapped and described in detail by El Ramly et al. (1969a). There are four major rock types: volcanics, gabbros (essexites), quartz syenites, and nepheline syenites. On the basis of field relations the oldest rocks were the volcanics which formed a pile unconformably overlying the basement gneisses and schists. The first intrusive rocks were the gabbros, emplaced in irregular masses beneath the volcanics. Syenites were then emplaced in several incomplete rings, decreasing in age toward the center. Early syenites were oversaturated to saturated while the latest, forming the core of the complex, were undersaturated. Previous K–Ar work (Serencsits et al. 1979) indicates that all intrusive units have ages of 89 Ma.

A continuous ring wadi separates the outer rings containing most of the quartz syenite from the inner ring of predominantly

nepheline syenite. El Ramly et al. (1969a) hypothesized that the ring wadi is the trace of a major ring fault; however, not enough is known about the stratigraphy of the volcanic sequence to establish the amount of subsidence, if any. The contacts between the syenites and the volcanics they intruded are exposed both inside and outside the ring wadi, suggesting that little relative movement occurred after emplacement of the syenites.

The "quartz syenites" contain alkali feldspar (58–86%), quartz (0–25%), alkali pyroxene (3–28%), and biotite (0–2%). The "nepheline syenites" contain alkali feldspar (50–83%), occasionally with plagioclase cores, nepheline (1–36%), analcime and sodalite (1–11%), alkali pyroxene (2–16%), and biotite (0–5%). Minor alkali amphibole, opaques, and apatite occur in both rock types. The essexites are less well known from our samples but typically consist of plagioclase (60%), biotite (20%), augite (10%), and opaques (5%) with minor apatite, amphibole, and olivine (El Ramly et al. 1969a). The modes of the samples analyzed are given in Table 1.

Abundant petrographic evidence demonstrates that the syenites and gabbro were affected by hydrothermal solutions. Feldspars are always cloudy and sometimes sericitized; nepheline is commonly altered to analcime or a fine-grained micaceous product (liebenerite), and quartz typically appears to be secondary. In the most quartz-rich samples (E-62, E-63) granophyric intergrowths of quartz and alkali feldspar suggest subsolidus replacement of feldspar by quartz, although late magmatic eutectic crystallization cannot be ruled out. However, the mineralogical alteration is not extreme: sericitization is not the rule and usually both alkali pyroxene and biotite have not been visibly affected. Low temperature hydrothermal phases that might garner Sr, such as calcite, were not observed in thin section.

Some samples of syenite, particularly those in the vicinity of the ring wadi, are iron-stained. In thin section the red stain is concentrated along planar zones in the feldspars, presumably in microfractures or in grain rims. In outcrop, the intensity of staining varies over distances of less than 100 m.

### Sampling and analytical procedures

Although overall exposure of rock at Abu Khruq is good the availability of fresh rock for isotopic analysis determined the sample

**Table 1.** Modal compositions of Abu Khruq syenites

Sample	F	P	Q	Ne	A	B
E-1	82	5	13			
E-11	86	3	10			
E-21	78	10	12			
E-22	83	12	2			2
E-23	86	12	0			1
E-29	69	28	2			
E-30	83	16	0			1
E-31	77	20	2			
E-61	83	12	5			
E-62	69	5	26			
E-63	58	15	27			
E-65	76	19	6			
E-2	64	13		21	1	
E-3	70	11		13	4	1
E-3a	69	13		14	1	3
E-5	56	9		33	2	
E-9	80	6		8	1	5
E-25	83	14		2	1	
E-26	68	15		15	3	
E-27	57	9		32	2	
E-28	63	16		16	5	
E-69	50	8		36	6	
E-70	52	8		26	11	
E-71	67	2		28	3	

F feldspar; P pyroxene; Q quartz; Ne nepheline; A analcime; B biotite

distribution (Fig. 1). The nepheline syenites were sampled fairly uniformly but the quartz syenites were taken primarily from a crescent-shaped mass in the north. The quartz syenites in the inner ring were collected from a small area on the western side.

Whole-rock samples of about 1 kg were crushed, a whole-rock split was taken, and the remainder was separated by standard techniques of mineral separation. Isotope dilution measurements for Rb and Sr and  $^{87}\text{Sr}/^{86}\text{Sr}$  analyses were made on 100–300 mg samples except in the case of some mineral separates when as little as 20 mg was dissolved.  $^{87}\text{Rb}$  and  $^{84}\text{Sr}$  spikes were added individually to each sample. The spiked samples were dissolved in concentrated HF and  $\text{HClO}_4$  prepared by non-boiling distillation. Rb was precipitated directly as an alkali chlorate; Sr was purified by ion exchange chromatography.

Isotopic ratio measurements were made at the University of Pennsylvania on a 30 cm, 68° NBS-type mass spectrometer operated on-line by minicomputer.  $^{87}\text{Sr}/^{86}\text{Sr}$  ratios were measured on the spiked samples; mass 85 was monitored to guard against isobaric  $^{87}\text{Rb}$  contamination. All Sr measurements were normalized to an  $^{86}\text{Sr}/^{88}\text{Sr}$  ratio calculated for the mixture of spike Sr (SRM 988) and normal Sr with an  $^{86}\text{Sr}/^{88}\text{Sr}$  ratio of 0.1194.

The  $^{87}\text{Rb}/^{86}\text{Sr}$  ratios have uncertainties of 0.75%;  $^{87}\text{Sr}/^{86}\text{Sr}$  ratios have uncertainties of about 0.02%. Blanks were insignificant for all analyses reported here. The  $^{87}\text{Sr}/^{86}\text{Sr}$  ratios are reported relative to a value of 0.71020 for the SRM 987 Sr isotope standard; relative to this value, ten analyses of the E & A standard gave an  $^{87}\text{Sr}/^{86}\text{Sr}$  of  $0.707983 \pm 0.000014$ .

Oxygen isotope analyses were performed at the isotope geology laboratories of the United States Geological Survey in Denver, Colorado. Oxygen was liberated by the method of Clayton and Mayeda (1963). Whole-rock and mineral samples of 10–20 mg were reacted with  $\text{BrF}_5$  at high temperature. Oxygen liberated was reacted quantitatively with a Pt-heated graphite rod to form  $\text{CO}_2$ , which was analyzed on a double-collector mass spectrometer. Uncertainties assigned to individual measurements of the  $^{18}\text{O}/^{16}\text{O}$  ratio are 0.1‰ (1 s.d.). Measurements are reported as delta values per mil with respect to the SMOW standard.

## Results

Rb and Sr concentrations and Sr and oxygen isotopic compositions of whole-rock and mineral samples are given in Table 2. The gabbros are characterized by high Sr concentrations (670–920 ppm). The syenites have lower, highly variable Sr concentrations: 7 ppm to 177 ppm in the quartz syenites and 9 ppm to 220 ppm in the nepheline syenites. Sr content is negatively correlated with modal proportion of quartz and nepheline as expected from magmatic differentiation (Table 3). Rb and Sr concentrations are negatively correlated in both syenite units (Fig. 3) with much of the variation originating as a result of differences between the stained and unstained samples.

The whole-rock Rb–Sr data from both units are shown on isochron diagrams in Fig. 2. The fit of each regression is statistically poor and neither slope is thought to reflect accurately the age of the samples. The initial ratios calculated at 89.5 Ma (see Discussion) range from 0.7028 (E-7) to 0.7031 (E-10) in the gabbros; from 0.7033 (E-11) to 0.7106 (E-63) in the quartz syenites; and from 0.7032 (E-9, E-25) to 0.7077 (E-70) in the nepheline syenites. The highest calculated initial ratio is 0.7163 for a nepheline separate from E-71. An anomalously low value of 0.6997 for a pyroxene separate from nepheline syenite E-3 evidently results from chemical alteration of the mineral, perhaps due to weathering. The whole-rock initial ratios are strongly correlated with Rb and Sr concentrations in both syenites (Table 3, Fig. 3).

The oxygen isotope compositions of the quartz syenites ( $\delta^{18}\text{O} = 4.5$  to 6.7‰) and gabbros ( $\delta^{18}\text{O} = 3.4$  to 4.2‰) are slightly depleted in  $^{18}\text{O}$  relative to “normal” rocks with their composition (Taylor 1974). The nepheline syenites ( $\delta^{18}\text{O} = 6.8$  to 9.0‰) are not depleted in  $^{18}\text{O}$  and some samples may be slightly enriched relative to “normal.” Rb and Sr concentrations are not well correlated with  $\delta^{18}\text{O}$  in either the quartz or nepheline syenites. A correlation between initial ratio and  $\delta^{18}\text{O}$  is well-developed only for the nepheline syenite samples (Table 3).

The patterns of Sr and oxygen isotopic variations among minerals within individual rock samples are consistent (Fig. 4). Most isotopic variations among samples of a single phase are relatively small. However, analcime separates are characterized by high and variable  $\delta^{18}\text{O}$  values (9.2–14.2‰) as might be expected from low temperature exchange of silicate with meteoric water.

## Discussion

### Age of the Abu Khruq intrusives

The ages of the intrusive units are based on K–Ar and Rb–Sr mineral data as summarized in Table 4. Serencsits et al. (1981) obtained K–Ar biotite ages of  $90 \pm 2$  Ma for gabbro (E-64) and  $89 \pm 2$  Ma for the nepheline syenite (E-3a). Rb–Sr data (Table 2) for these same biotites yield ages of  $89 \pm 4$  Ma (gabbro) and  $87 \pm 2$  Ma (nepheline syenite). Thus, biotites from the oldest and youngest intrusions give concordant Rb–Sr and K–Ar ages which are interpreted as dating the time of emplacement and crystallization of this small, shallow intrusive complex.

Mineral Rb–Sr data for a quartz syenite (E-21) and two nepheline syenites (E-3a, E-69) yield regression ages of  $92 \pm 2$  Ma,  $88 \pm 2$  Ma, and  $93 \pm 6$  Ma and are in agree-

**Table 2.** Rb—Sr and oxygen isotope data for rock and mineral samples from Abu Khruq

Sample	ppm Rb	ppm Sr	$^{87}\text{Rb}/^{86}\text{Sr}$	$^{87}\text{Sr}/^{86}\text{Sr}$	$(^{87}\text{Sr}/^{86}\text{Sr})_0$	$\delta^{18}\text{O}$
Nepheline syenites						
E-2 R	104.2	12.57	24.00	0.73535 (5)	0.70483 (23)	6.3
E-3 R	103.7	49.56	6.056	0.71226 (4)	0.70456 (7)	8.3
F wh	98.99	10.89	26.30	0.73815 (6)	0.70740 (26)	
F r	72.08	37.79	5.519	0.71235 (5)	0.70533 (7)	
P	85.31	22.40	11.02	0.71371 (8)	0.69969 (13)	
E-3a R	117.3	9.37	36.227	0.75304 (14)	0.70697 (37)	7.7
F	113.5	7.15	45.926	0.76506 (26)	0.70666 (51)	7.5
B	523.0	1.22	1235.0	2.2343 (9)		2.5
N	62.95	17.19	10.59	0.72152 (7)	0.70805 (12)	
A	11.84	10.99	3.116	0.71084 (21)	0.70688 (21)	11.4
E-5 R	98.87	11.64	24.58	0.73700 (15)	0.70575 (28)	7.6
E-9 R	79.27	223.1	1.028	0.70453 (2)	0.70322 (2)	7.2
E-25 R	49.59	77.45	1.853	0.70557 (5)	0.70321 (5)	6.7
F 1	44.86	113.5	1.144	0.70434 (3)	0.70289 (3)	6.3
F 2	58.40	60.25	2.805	0.70668 (3)	0.70311 (4)	7.3
E-26 R	124.9	44.31	8.156	0.71738 (10)	0.70701 (13)	8.6
E-27 R	113.2	28.97	11.31	0.72100 (8)	0.70661 (13)	9.0
F						7.6
A	23.07	61.33	1.089	0.70701 (4)	0.70563 (4)	14.2
E-28 R	161.2	23.14	20.15	0.73098 (12)	0.70535 (13)	7.7
F	210.1	26.04	23.35	0.73402 (3)	0.70432 (22)	7.7
A	62.59	24.88	7.280	0.71533 (3)	0.70607 (8)	11.1
E-69 R	88.15	13.53	18.86	0.72984 (7)	0.70585 (19)	8.7
F						8.1
P	24.16	6.62	10.56	0.71678 (5)	0.70334 (11)	4.8
N	84.20	8.10	30.09	0.74581 (4)	0.70754 (29)	9.0
A	9.84	17.25	1.651	0.70741 (5)	0.70531 (5)	13.3
E-70 R	121.0	23.79	14.72	0.72640 (10)	0.70767 (17)	9.0
E-71 R	98.50	10.52	27.09	0.74102 (8)	0.70657 (27)	8.7, 9.1
F						8.1
N	91.09	3.69	71.34	0.80703 (15)	0.71631 (70)	8.2
A						9.2
Quartz syenites						
E-1 R	88.44	16.13	15.88	0.72742 (4)	0.70723 (16)	4.7
Q						4.8
F						4.2
E-11 R	84.96	177.5	1.385	0.70501 (3)	0.70326 (3)	6.4
E-21 R	88.67	18.01	14.25	0.72410 (7)	0.70597 (15)	4.5
Q						5.5
F	103.4	13.27	22.54	0.73434 (10)	0.70658 (24)	4.4
P	7.23	12.97	1.613	0.70734 (8)	0.70529 (8)	1.7
M						1.9
E-22 R	57.69	67.85	2.461	0.70729 (9)	0.70416 (9)	5.5
Q						6.5, 6.4
F	84.32	29.38	8.304	0.71548 (3)	0.70492 (8)	5.6
F wh	82.11	14.59	16.28	0.72628 (4)	0.70558 (16)	
F r	63.55	109.7	1.676	0.70574 (5)	0.70361 (5)	
P	4.73	31.81	0.4299	0.70511 (5)	0.70456 (5)	3.4
E-23 R	88.43	26.54	9.641	0.71640 (7)	0.70414 (12)	6.6
F						6.6
E-29 R	78.64	15.04	15.13	0.72504 (5)	0.70579 (15)	5.6
E-30 R	49.94	100.9	1.432	0.70513 (4)	0.70331 (4)	5.6
F						5.6
M						0.6
E-31 R	54.45	32.41	4.862	0.71034 (4)	0.70416 (6)	4.8
F						4.1

**Table 2** (continued)

Sample		ppm Rb	ppm Sr	$^{87}\text{Rb}/^{86}\text{Sr}$	$^{87}\text{Sr}/^{86}\text{Sr}$	$(^{87}\text{Sr}/^{86}\text{Sr})_0$	$\delta^{18}\text{O}$
Quartz syenites							
E-61	R	84.57	10.37	23.60	0.73748 (7)	0.70747 (24)	4.5
	Q						4.8, 5.9
	F						3.8
	P						1.8
E-62	R	107.5	7.75	40.14	0.76036 (12)	0.70932 (40)	5.8, 6.1
	Q						6.3, 6.5
	F	148.7	6.41	67.16	0.79615 (3)	0.71075 (64)	5.7
E-63	R	149.7	6.70	64.67	0.79282 (7)	0.71058 (62)	4.8
	Q						5.5, 5.5
	P	14.81	7.39	5.803	0.71349 (12)	0.70611 (13)	5.3, 5.5
E-65	R	51.42	25.14	5.919	0.71319 (3)	0.70566 (6)	4.3
	Q						6.7
	P						6.4, 7.0
							4.9
Essexite gabbros							
E-7	R	16.82	919.0	0.05297	0.70292 (4)	0.70285 (4)	4.2
	F						4.5
E-10	R	12.56	904.2	0.04019	0.70316 (4)	0.70311 (4)	3.4
	F						5.3
	P	3.33	44.43	0.2168	0.70341 (4)	0.70313 (4)	4.9
E-64	R	13.91	668.1	0.06027	0.70301 (15)	0.70293 (15)	3.7, 3.4
	B	189.5	61.91	8.857	0.71411 (13)	0.70285 (16)	1.3

Initial  $^{87}\text{Sr}/^{86}\text{Sr}$  ratios calculated assuming an age of 89.5 Ma and a  $^{87}\text{Rb}$  decay constant of  $1.42 \times 10^{-11} \text{ y}^{-1}$ . Uncertainties are estimated at the one standard deviation level, and the uncertainty in initial ratio includes a 0.75% uncertainty in the  $^{87}\text{Rb}/^{86}\text{Sr}$  ratio. Sample types: *R* rock; *Q* quartz; *F* feldspar [*r* "red" (stained), *w* "white" (unstained)]; *P* pyroxene; *N* nepheline; *A* analcime; *B* biotite; *M* magnetite. Oxygen values are given relative to the SMOW standard

**Table 3.** Spearman rank correlation coefficients (Kendall 1975)

Quartz syenites					
	Rb	Sr	$(^{87}\text{Sr}/^{86}\text{Sr})_0$	$^{18}\text{O}$	Q
Rb	1	-0.62	0.69	-0.04	0.70
Sr	-0.62	1	-0.95	0.27	-0.59
$(^{87}\text{Sr}/^{86}\text{Sr})_0$	0.69	-0.95	1	-0.26	0.74
$^{18}\text{O}$	-0.04	0.27	-0.26	1	-0.13
Q	0.70	-0.59	0.74	-0.13	1
Nepheline syenites					
	Rb	Sr	$(^{87}\text{Sr}/^{86}\text{Sr})_0$	$^{18}\text{O}$	Ne
Rb	1	-0.20	0.63	0.35	0.09
Sr	-0.20	1	-0.49	-0.12	-0.50
$(^{87}\text{Sr}/^{86}\text{Sr})_0$	0.63	-0.49	1	0.71	0.46
$^{18}\text{O}$	0.35	-0.12	0.71	1	0.54
Ne	0.09	-0.50	0.46	0.54	1

The 95% critical region for both quartz and nepheline syenites is  $r_s = 0.497$ .  $(^{87}\text{Sr}/^{86}\text{Sr})_0$  refers to the calculated initial  $^{87}\text{Sr}/^{86}\text{Sr}$  ratio; *Q* and *Ne* refer, respectively, to modal quartz and nepheline content

ment with the K—Ar and Rb—Sr biotite ages. However, the indicated initial  $^{87}\text{Sr}/^{86}\text{Sr}$  ratios (0.7053, 0.7075, 0.7045) are distinctly higher than the intercepts of the whole-rock data (0.7035, 0.7039; see below). In sample E-21 the whole-

rock  $\delta^{18}\text{O}$  (4.5‰) is low relative to normal values, suggesting interaction with meteoric water, and the mineral fractionations (Table 2) indicate approximate oxygen isotopic equilibrium at or just below magmatic temperatures. These data document Sr isotopic heterogeneity among rock samples, as well as Sr isotopic homogeneity among coexisting minerals in some rocks, at the time of crystallization.

It is unlikely that this consistent pattern of biotite mineral ages and Rb—Sr mineral isochrons involving biotite, feldspar, analcime, nepheline, and pyroxene are the result of resetting substantially (several m.y.) after emplacement of the Abu Khruq magmas. Instead, the data suggest that all the units were emplaced within a short period of time and cooled quickly, an interpretation supported by the low temperature cooling history of Abu Khruq and the basement complex revealed by fission track dates (Omar et al. 1987). For the discussion below, an age of 89.5 Ma is assigned to all units for the purpose of calculating initial  $^{87}\text{Sr}/^{86}\text{Sr}$  ratios.

The Rb—Sr whole-rock data (Fig. 2) do not define acceptable isochrons because they show extreme scatter about the best fit regression lines. The regressions yield ages of about 100 Ma for both the quartz and nepheline syenites but the MSWD values (Brooks et al. 1972) of 16 and 47, respectively, indicate gross "geological error." Moreover, these apparent "ages" are much too old relative to Rb—Sr and K—Ar mineral dates which indicate a crystallization age of about 89 Ma. The anomalously high whole-rock ages are an example of systematic age shifts (Lutz and Srogi 1986) that resulted from Sr isotopic heterogeneity among

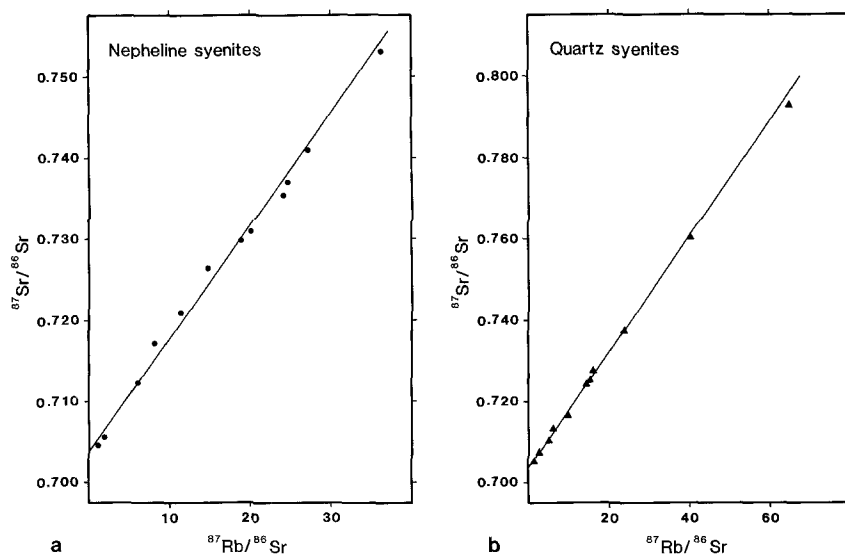


Fig. 2 a, b. Isochron diagrams for whole-rock data for nepheline syenites (a) and quartz syenites (b) (Table 2). "Ages" and initial ratios (Table 4) were determined using the procedure of York (1969). The scatter of the data about the regressions greatly exceeds experimental error, as described in the text

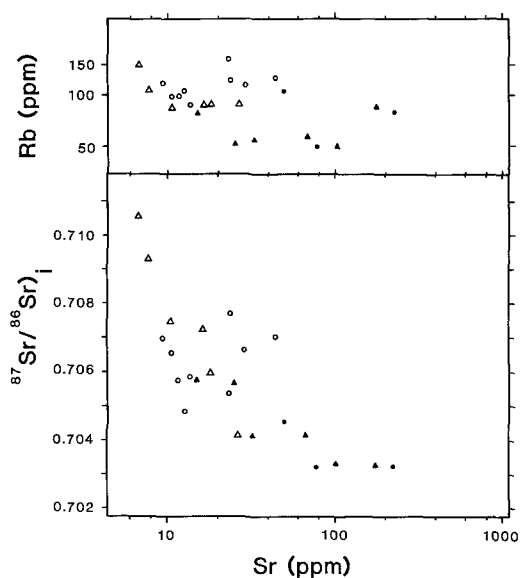


Fig. 3. Variation of Rb concentration and initial  $^{87}\text{Sr}/^{86}\text{Sr}$  ratio vs. Sr concentration. Initial ratios are calculated for an age of 89.5 m.y. Triangles represent quartz syenites; circles nepheline syenites. Open and filled symbols represent unstained and red-stained samples, respectively. The stained samples systematically have higher Sr concentrations and lower  $^{87}\text{Sr}/^{86}\text{Sr}$  ratios

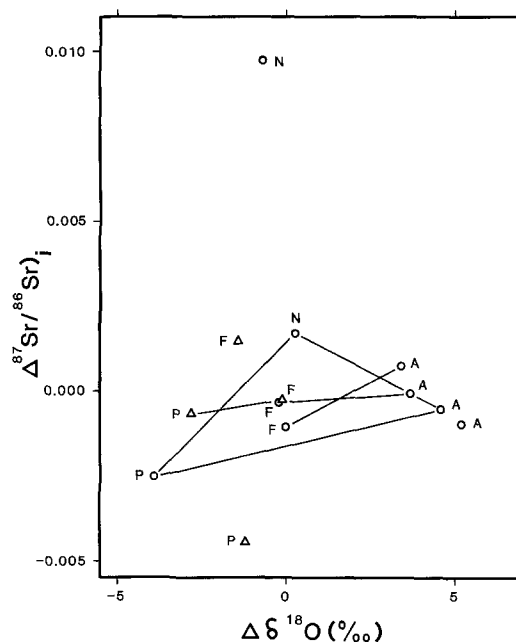


Fig. 4. Deviations in the Sr and O isotopic compositions of minerals relative to the composition of the rocks in which they are found. Symbols as in Fig. 3; letter codes as in Table 2. Minerals co-existing in the same rock sample are connected by lines

whole-rock samples produced by hydrothermal alteration at the time of emplacement.

In summary, the intrusive units of the Abu Khruq complex were emplaced within a short time 89.5 Ma ago. In the remainder of the discussion " $^{87}\text{Sr}/^{86}\text{Sr}$  ratio" will refer to the initial Sr isotopic composition calculated for 89.5 Ma ago.

#### Causes of isotopic heterogeneity

Heterogeneity of initial Sr isotopic composition among minerals in the same rock sample is common for the Abu Khruq syenites (Fig. 4). Pyroxenes in both the quartz and nepheline syenites have the lowest initial ratios for phases

within individual samples. Feldspars have initial ratios greater than pyroxenes but lower than analcime or nepheline, where present. These isotopic heterogeneities could have resulted either from a change in the isotopic composition of the magma during crystallization (e.g., progressive assimilation) or from alteration of the rock after crystallization (e.g., subsolidus hydrothermal alteration). In the former case one expects that intermineral heterogeneities will be correlated with the order in which phases crystallize from the melt. The chemical compositions of the syenites within petrogeny's residua system suggest that feldspar was the earliest crystallizing phase and that nepheline crystallized together with feldspar. Pyroxene is xenomorphic with respect to feldspar and nepheline, in accord with the obser-

**Table 4.** Summary of geochronologic estimates for Abu Khruq rock units

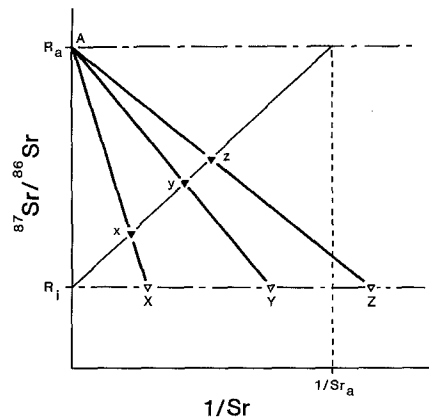
Data	Age (Ma)	$^{87}\text{Sr}/^{86}\text{Sr}$ intercept	Source
<b>Gabbro</b>			
Rb—Sr E-64/R, B	$89 \pm 2$	0.70293 (15)	1
K—Ar E-64/B	$90 \pm 2$		2
<b>Quartz syenite</b>			
Rb—Sr 12 R	$100 \pm 2$	0.70354 (29)	1
E-21/R, F, P	$92 \pm 2$	0.70529 (27)	1
F—T E-11/Z	$90 \pm 4$		3
<b>Nepheline syenite</b>			
Rb—Sr 12 R	$98 \pm 3$	0.70392 (60)	1
E-3a/R, F, N, A, B	$88 \pm 2$	0.70746 (44)	1
E-69/R, N, A, P	$93 \pm 6$	0.70448 (118)	1
K—Ar E-3a/B	$89 \pm 2$		2

R whole rock; B biotite; F feldspar; P pyroxene; N nepheline; A analcime; Z zircon. All ages calculated with an  $^{87}\text{Rb}$  decay constant of  $1.42 \times 10^{-11} \text{ y}^{-1}$  and the K—Ar constants given by Steiger and Jäger (1977). Rb—Sr regressions follow York (1969). The fission track age is calculated using a fission decay constant for  $^{238}\text{U}$  of  $7.03 \times 10^{-17} \text{ y}^{-1}$ . References: 1 This study; 2 Serencsits et al. (1981); 3 Omar et al. (1987)

vation that alkali pyroxene is a late crystallizing phase in alkaline syenites (Deer et al. 1966). Magmatic assimilation cannot explain differential contamination of feldspar and nepheline together with consistently low initial ratios in late pyroxene.

A characteristic feature of subsolidus alteration is that its effect and degree is a function of the modal composition of the rock because minerals have different susceptibilities to hydrothermal alteration, different grain sizes, and different concentrations of Sr and other trace elements. Low  $^{87}\text{Sr}/^{86}\text{Sr}$  ratios are typical of fresh pyroxene while higher ratios are typical of more altered feldspar, and the highest ratios are found for the most altered phase, nepheline. This pattern, along with other evidence of subsolidus alteration, indicates that hydrothermal modification was a major cause of Sr and oxygen isotopic variation. The most simple explanation of intermineral isotopic variations is that both syenite magmas had low  $^{87}\text{Sr}/^{86}\text{Sr}$  ratios and that contamination by radiogenic Sr after crystallization was controlled by the susceptibilities of the minerals to alteration by circulating meteoric waters. However, because of the hydrothermal alteration it is impossible to ascertain whether assimilation caused minor isotopic heterogeneities.

In addition to Sr isotopic heterogeneity among different minerals there are also variations in initial Sr ratio within individual mineral grains (as explained below). These are interpreted in terms of a progressive decrease in the size of domains over which isotopic equilibration or exchange took place during hydrothermal modification. The smaller domains reflect lower temperatures of the later stages of hydrothermal activity. In order to facilitate discussion, "first stage" and "second stage" will be used to refer to the chemical and isotopic characteristics associated with intermineral and intramineral variations, respectively. It cannot be demonstrated, nor is it suggested, that there were actually two distinct stages of hydrothermal alteration.

**Fig. 5.** Schematic diagram showing the systematics of Sr addition as defined in the text

The unstained syenites are interpreted as rocks that were affected only by the first stage of alteration. The isotopic data show that this stage occurred pervasively while the second stage only overprints the first in stained samples. The stained rocks developed when the pathways for fluid migration were no longer penetrative on the scale of rock samples and thus even samples close to one another were affected differently. The second stage developed primarily close to major structural contacts: the ring wadi and the contact of the intrusive rocks with the country rocks.

#### The addition model

To facilitate the discussion of the variations of Sr concentration and isotopic composition among rock samples and within minerals we assume that the solutions which interacted with the syenites acted as reservoirs of Sr and that the minerals, except quartz, acted as sinks for Sr. Realistically, the situation must have been more complicated and probably involved two-way exchange. However, the coupled changes in Sr concentration and isotopic composition caused by hydrothermal solutions at Abu Khruq can be explained by one-way exchange. More complicated models of exchange would yield second-order effects that the data are insufficient to test adequately. The simple model is called an *addition* model and is an alternative to a one-to-one exchange reaction model which is often assumed for oxygen isotope exchange.

The effects of Sr addition on Rb—Sr isochron relationships have been considered in detail by Lutz and Srogi (1986), and will not be reiterated here. However, the effects of Sr addition on the systematics of initial ratio vs.  $1/\text{Sr}$  diagrams are developed below. Rb mobility plays no role in the systematics in either case because the alteration occurred simultaneously with formation of the Rb—Sr systems.

Changes in  $^{87}\text{Sr}/^{86}\text{Sr}$  ratio and Sr concentration as a result of addition of Sr can be shown by plotting  $^{87}\text{Sr}/^{86}\text{Sr}$  ratio versus the reciprocal of Sr concentration,  $1/\text{Sr}$ , as shown in Fig. 5. Points X, Y, and Z (open symbols) represent initial rocks with the same original  $^{87}\text{Sr}/^{86}\text{Sr}$  ratio ( $R_i$ ) but different Sr concentrations. Adding Sr with a constant composition  $R_a$  will cause the rocks to plot along trajectories similar to X-A in Fig. 5, and the distance along each trajectory will be determined by the amount of Sr added ( $Sr_a$ ). Lines of equal  $Sr_a$  for a fixed  $R_a$  must all pass through the point ( $1/\text{Sr}=0$ ,  $R=R_i$ ); their slopes will be given by

$Sr_a \cdot (R_a - R_i)$ . If X, Y, and Z take up the same amount of Sr they will plot as collinear points x, y, and z (closed symbols). The value of  $Sr_a$  for any sample can be estimated from the intersection of a line through the sample point and  $(1/Sr=0, R=R_i)$  with the line  $R=R_a$ . Points for samples that have experienced addition of different amounts of Sr will form a fan that will delimit the range of  $Sr_a$ . The amount added may be expressed as a ppm increase in concentration.

#### First stage addition

Minerals in the unstained syenites are typically out of isotopic equilibrium and the most easily altered minerals have the highest  $^{87}Sr/^{86}Sr$  ratios as discussed above and shown in Fig. 4. Among the few samples in which minerals appear to have equilibrated isotopically, the initial ratios are high and variable (Table 4). The amount of Sr added, on average, during the first stage can be estimated from the original isotopic composition of the rocks ( $R_i$ ) and the isotopic composition of the added Sr ( $R_a$ ). The initial ratio intercepts of the whole-rock regressions provide an estimate of  $R_i$ . The York (1969) regression model is used for this purpose since more sophisticated "error-chron" treatments are predicated on the assumption of a normal distribution of "geological error" (Brooks et al. 1972) that cannot be justified here. The initial ratios of the quartz and nepheline syenites are statistically indistinguishable (Table 4) and average 0.7037. This value is only slightly higher than the initial ratio of about 0.7030 implied by the cogenetic gabbros.

The highest calculated initial ratio of 0.716 for a nepheline separate from E-71 sets a lower limit on  $R_a$ . Although  $R_a$  might have been higher or even varied, choosing this lower limit yields the maximum estimates of the amount of Sr added ( $Sr_a$ ). The  $^{87}Sr/^{86}Sr$  ratio of the added Sr ( $R_a$ ) is higher than the original  $^{87}Sr/^{86}Sr$  ratio of any rock type within the Abu Khruq complex and Sr with this composition could have been derived from the Precambrian granitic gneisses and schists of the basement complex.

Only data from the unstained syenites are used to calculate  $Sr_a$ , as illustrated in Fig. 6. Values of  $Sr_a$  for individual samples range from 2 ppm to 13 ppm with an average of about 5 ppm. Although the changes in Sr concentrations were slight, the effects of Sr addition on isochron regression relations were important. The model of Lutz and Srogi (1986) suggests that regression of the whole-rock Rb—Sr data could yield an age 10 m.y. too old, as suggested by the difference between the mineral and whole-rock data.

The oxygen isotopic fractionations between minerals in the unstained syenites are also variable. For example, in the quartz syenites the fractionation between quartz and feldspar varies from virtually 0‰ (E-63) to 1.1‰ (E-21); and quartz-pyroxene fractionations vary from 1.1‰ (E-63) to 3.8‰ (E-21). These differences may reflect different temperatures of equilibration and different time-integrated water/rock ratios. However, intramineral heterogeneities occur in some of these mineral separates and any estimate of the water/rock ratios or paleotemperatures based on these data would have large uncertainties.

#### Second stage addition

In contrast to the pattern of intermineral variation of  $^{87}Sr/^{86}Sr$  ratios outlined above, intramineral variations sug-

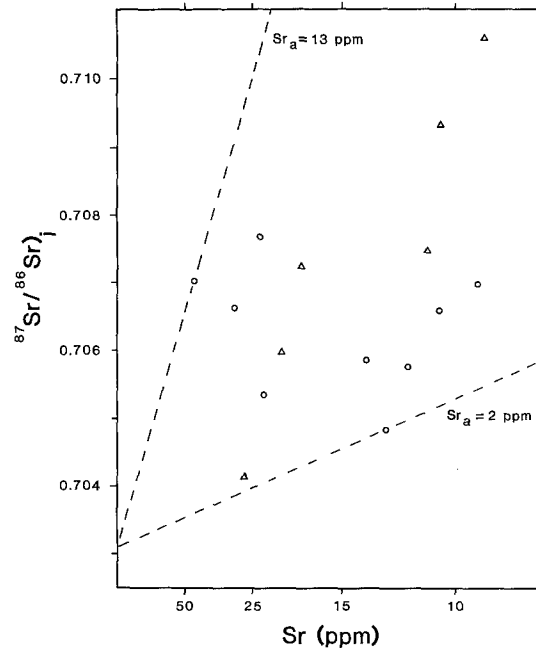


Fig. 6. Sr addition diagram for unstained syenites. The Sr concentration of the rocks is plotted to be linear in  $1/Sr$  as in Fig. 5. Symbols as in Fig. 3. The limiting amounts of added Sr are based on the assumption that the unaltered initial  $^{87}Sr/^{86}Sr$  ratio of the syenites was 0.7037 and that the  $^{87}Sr/^{86}Sr$  ratio of the added Sr was 0.716 (see text)

gest that Sr with a lower  $^{87}Sr/^{86}Sr$  ratio was strongly partitioned into the rocks later in their hydrothermal history. The change in the isotopic composition of the added Sr was probably gradual as suggested by variations in the isotopic compositions of the more altered portions of minerals from stained rocks.

*Permeability-controlled alteration: stained vs. unstained samples.* Portions of feldspar grains from a stained syenite (E-22) were handpicked to form a "red" and a "white" separate. The stained portions of the grains have Sr concentrations more than seven times higher than the unstained portions (109.7 ppm vs. 14.6 ppm) and much lower initial ratios (0.7036 vs. 0.7056). Rb concentrations are lower in the stained separate (63.5 ppm vs. 82.1 ppm). Several other comparisons can also be made with analogous samples showing this general pattern. Analyses of stained and unstained feldspar separates from E-3 show that "red" has a higher concentration of Sr than "white" (37.8 ppm vs. 10.9 ppm), a higher initial ratio (0.7053 vs. 0.7047), and a lower concentration of Rb (72.1 ppm vs. 99.0 ppm). The pattern of Sr enrichment and Rb depletion is identical to that in E-22 feldspars. A higher initial ratio in the E-3 "red" feldspar may have resulted from a gradual change in Sr isotopic of the hydrothermal fluid from high  $^{87}Sr/^{86}Sr$  ratios to lower ratios over time.

A similar relationship to that between stained and unstained feldspars is found between albite rims and perthite cores in a nepheline syenite (E-25). The rims have more Sr (113.5 ppm vs. 60.25 ppm), a marginally lower initial ratio (0.7029 vs. 0.7031), and less Rb (44.9 ppm vs. 58.4 ppm). The development of the albite rim by subsolidus rather than magmatic crystallization is suggested by a different  $\delta^{18}O$  in the rims than in the cores (6.3‰ vs. 7.3‰).



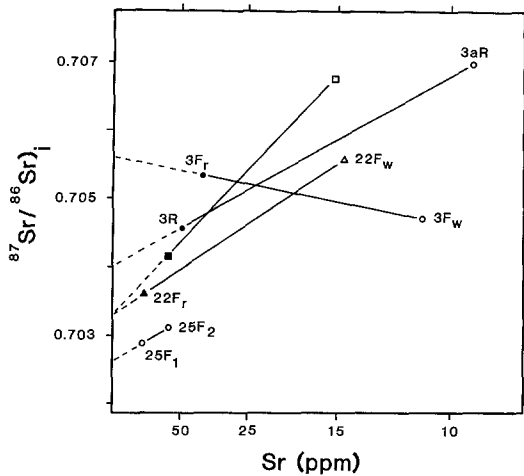


**Fig. 7.** Sr addition diagram for stained and unstained pairs of samples to estimate the composition of added Sr during the second stage. Symbols as in Fig. 3; letter codes as in Table 2; subscripts indicate white (unstained) or red (stained) samples. For example,  $3F_w$  is unstained feldspar from E-3,  $25F_1$  and  $25F_2$  are explained in the text. The square symbols indicate averages for stained and unstained whole-rock samples

The whole-rock sample has a slight red stain although none could be recognized in either feldspar separate.

The pattern of mineral heterogeneities suggests that stained rock samples are systematically different from unstained ones. A direct comparison can be made for E-3 and E-3a. These samples were collected from a spoil heap at the end of a short adit and in situ they were probably within 100 m of one another. They have nearly identical modes (Table 1) but E-3 is stained while E-3a is not. E-3 contains five times more Sr (49.6 ppm vs. 9.4 ppm), less Rb (103.7 ppm vs. 117.3 ppm), and a lower initial ratio (0.7046 vs. 0.7070) than E-3a. Stained syenites as a group contain, on average, 38 ppm less Rb, 46 ppm more Sr, and have a lower initial ratio (0.7041 vs. 0.7067). (To compare stained and unstained samples the logs of the concentrations are used because these data more closely follow a lognormal rather than a normal distribution.)

The isotopic composition of Sr added during the second stage can be estimated using the addition model (Fig. 7). The range of  $R_a$  inferred (0.7026 to 0.7056) is substantial but  $R_a$  was obviously lower than required by the first stage. A range might be expected because staining need not only have accompanied addition of Sr with the very lowest  $^{87}\text{Sr}/^{86}\text{Sr}$  ratio. The amount of Sr added cannot be estimated directly but the difference in average Sr concentration between stained and unstained syenites suggests that  $Sr_a$  may have averaged 45 ppm.

The relatively large amount of added Sr with a low  $^{87}\text{Sr}/^{86}\text{Sr}$  ratio combined with the restricted spatial distribution of the stained rocks suggest that the essexite gabbros within the Abu Khruq complex were the source of most of the Sr added during the second stage. The gabbros have an average initial ratio of 0.7030 and were little affected by the first stage addition of radiogenic Sr because of their high Sr concentrations (830 ppm on average). Enhanced mobility of Sr derived from gabbros during the second stage was probably related to formation of, or additional movement on, ring faults along which the gabbros and stained syenites crop out.

Large changes in Sr concentration during the second stage had little further effect on the Rb–Sr isochron systematics because the added Sr had an isotopic composition similar to the original isotopic composition of the syenites. A similar situation is described by Criss and Fleck (1987) for rocks in the Bitterroot lobe of the Idaho batholith. There the external sources of Sr were isotopically similar to the original compositions of the rocks being emplaced.

Second-stage hydrothermal alteration was heterogeneous and confined to zones of enhanced permeability as revealed by staining. On a large-scale, these zones developed close to fractures and ring faults. Within affected rocks, staining of mineral grains (indicating permeable zones) was associated with microfractures and grain boundaries.

*Mineralogically-controlled alteration: quartz vs. nepheline syenites.* Despite marked differences in mineralogy, both quartz and nepheline syenites have similar chemical characteristics. For example, both syenite types have positive correlations between Rb concentration and  $^{87}\text{Sr}/^{86}\text{Sr}$  ratio and negative correlations between Sr concentration and  $^{87}\text{Sr}/^{86}\text{Sr}$  ratio. However, plots of Rb vs. Sr and Sr vs. initial ratio (Fig. 3) show that these correlations result largely from variation between stained and unstained samples, as discussed above. The similarity of Rb–Sr behavior in both syenite types is due to the abundance of feldspar, which makes up from 50% to 86% of the mode. Most of the Rb and Sr in the syenites is contained in feldspar; thus, alteration of feldspar grains largely controlled the Rb–Sr variations. Magmatic differentiation also played a role in the behavior of Rb and Sr, as suggested by significant negative correlations of Sr concentration with proportion of modal quartz and nepheline (Table 3).

The quartz and nepheline syenites differ with regard to correlation of  $\delta^{18}\text{O}$  values and initial  $^{87}\text{Sr}/^{86}\text{Sr}$  ratios: a significant correlation exists only for the nepheline syenites. Nepheline consistently has the highest calculated initial ratio of minerals in the nepheline syenites and was evidently highly susceptible to Sr exchange. In addition, nepheline reacted at low temperatures to form  $^{18}\text{O}$ -enriched analcime and there is a positive correlation between proportions of modal analcime and modal nepheline ( $r_s=0.48$ ). Essentially, the initial modal proportion of a single primary phase, nepheline, affected the Sr and O isotopic alteration to a significant extent. In contrast, there is no corresponding phase in the quartz syenites: quartz accounts for a substantial portion of the oxygen budget but has a negligible effect on the Sr budget. Clearly, mineralogy plays an important role in either augmenting or diminishing the decoupling of trace element and oxygen isotopic alteration.

#### *Intramineral heterogeneity in $\delta^{18}\text{O}$*

Two quartz separates from each of two samples (E-61, E-65) were prepared with different purities (98% and >99%). In each case the purer sample was significantly enriched in  $^{18}\text{O}$ , in the case of E-61 by 1.1 per mil. The difference in  $^{18}\text{O}/^{16}\text{O}$  ratios cannot be explained by removal of any impurity: its isotopic composition would have to be far outside the range of naturally occurring  $^{18}\text{O}/^{16}\text{O}$  ratios in minerals. The rims of mineral grains are preferentially incorporated in compound particles with adjacent phases when the rock is disaggregated. Removing compound particles from a separate, therefore, depletes it in grain rims.

The differences between quartz separates indicates a rim of  $^{18}\text{O}$ -depleted quartz which formed by exchange with hydrothermal solutions at high temperatures.

Further evidence of oxygen isotopic heterogeneity comes from samples E-62 and E-63. The measured quartz-feldspar fractionations are positive and since these rocks consist mostly of feldspar it would be expected that the whole-rock  $\delta^{18}\text{O}$  should be greater than  $\delta^{18}\text{O}$  of feldspar but close to it. However, the  $\delta^{18}\text{O}$  of the rock samples in both cases is greater than or equal to that of the quartz separates from the same rocks. Therefore, some important fractionation and loss of  $^{18}\text{O}$ -rich grain rims must have occurred during the mineral separation process. The large variation of  $\delta^{18}\text{O}$  among four replicate analyses of E-62 might also be explained by the presence of extreme, fine-scale heterogeneity in the rock sample considering the small (10–20 mg) samples analyzed.

Statistically, there are no significant differences in  $\delta^{18}\text{O}$  between stained and unstained rock samples or between feldspar separates from stained and unstained samples (Fig. 4). The scale of oxygen isotope exchange was evidently limited at the temperatures at which the second stage alteration occurred. Therefore, the differences between the  $\delta^{18}\text{O}$  values of the quartz and nepheline syenites predated the second stage of alteration. This suggests that the large changes in Sr concentration and isotopic composition during the second stage were nearly independent of changes in oxygen isotope composition of the rocks.

Some of the differences in oxygen isotopic composition between quartz and nepheline syenites may be related to specific differences in mineralogy: analcime in nepheline syenites may have  $\delta^{18}\text{O}$  values as high as 14.2‰ (E-27), while no similarly enriched phase exists in the quartz syenites. However, the small amounts of analcime observed in thin section, averaging about 3%, cannot account for the entire difference. Some differences are clearly not related to analcime:  $\delta^{18}\text{O}$  values of feldspar separates from unstained nepheline syenites average 7.8‰ while those from unstained quartz syenites average 4.8‰. Three factors, or some combination of them, could be responsible for the differences between the feldspars: 1) the quartz and nepheline syenite magmas had different  $^{18}\text{O}/^{16}\text{O}$  ratios; 2) the quartz syenite experienced more alteration because it was emplaced before the nepheline syenite; or 3) the units were affected by hydrothermal solutions with different oxygen isotopic compositions. The data are insufficient to adequately test any of these hypotheses, however.

#### *Summary of hydrothermal effects*

The Abu Khruq intrusives experienced hydrothermal alteration typical of epizonal rocks: the feldspars are cloudy and sometimes sericitized and nepheline has been partially altered to analcime. The quartz syenite and gabbro are slightly depleted in  $^{18}\text{O}$  as a result of high temperature interaction with meteoric water at the time the rocks formed. The nepheline syenite has nearly “normal”  $\delta^{18}\text{O}$  values, but anomalously “heavy” analcime suggests that the whole-rock  $\delta^{18}\text{O}$  values resulted from compensating effects of both high- and low-temperature alteration. The overall degree of alteration of mineralogy and whole-rock oxygen isotopic compositions at Abu Khruq is not extreme.

Chemical and isotopic variations related to hydrothermal alteration are observed on three different scales: among

rock samples, among the mineral species within rock samples, and within mineral grains. Intramineral variations are superimposed on intermineral variations and suggest that the effects of alteration were not uniform, reflecting, among other things, a change in the source of Sr carried in solution.

The susceptibilities of the minerals to alteration were important factors causing isotopic heterogeneities. Consistent patterns of disequilibrium suggest that radiogenic Sr was added to the syenites during the first stage of alteration. The country rocks were the only conceivable sources for Sr with a high  $^{87}\text{Sr}/^{86}\text{Sr}$  ratio 89.5 Ma ago and thus the scale of Sr transport must have been on the order of kilometers. However, since minerals within most rock samples did not equilibrate the scale of equilibration must have been much smaller, on the order of centimeters, or less.

The average change in Sr concentrations of rock samples during the first stage was only about 5 ppm but there were nevertheless significant effects. The most important was a systematic change in Sr concentration and  $^{87}\text{Sr}/^{86}\text{Sr}$  ratio at the time of alteration which had the effect of increasing the apparent Rb–Sr whole-rock age of the syenites.

The second stage of alteration is observed in both quartz and nepheline syenites located near the major ring fractures where fluids could percolate most easily through faulted rock. Increases in Sr concentrations and decreases in Rb concentrations and  $^{87}\text{Sr}/^{86}\text{Sr}$  ratios occurred in portions of minerals along grain boundaries or microfractures. Fortunately, portions of rocks and minerals affected during this stage have iron stains: the superposition of low temperature effects on high temperature effects would not have been recognized otherwise. The source of Sr in the hydrothermal solutions during the second stage was the gabbro unit which crops out close to the ring fractures.

During the second-stage alteration, Sr and oxygen isotopic compositions were decoupled: Sr added to grain rims changed the whole-rock Rb–Sr systematics significantly whereas modification of oxygen isotopic compositions within rims had little effect on the rocks. Thus, the whole-rock  $\delta^{18}\text{O}$  values are not consistently well correlated with Rb or Sr concentrations in either the quartz or nepheline syenites. Oxygen isotopic compositions of whole-rock samples are not good measures of trace element and Sr isotopic alteration at Abu Khruq.

#### **Conclusions**

Common effects of hydrothermal alteration associated with continental igneous rocks are replacement of primary anhydrous mineralogies by hydrous assemblages, ore mineralization, or depletions (high temperature) or enrichments (low temperature) in  $^{18}\text{O}$ . Accordingly, some studies have assumed that extreme alterations of igneous chemistry should be associated with extreme mineralogic or oxygen isotopic alteration, and that the absence of correlations between chemical, isotopic, and mineralogic compositions indicate that hydrothermal alteration did not affect the igneous chemistry.

The results from Abu Khruq suggest that correlations between  $\delta^{18}\text{O}$  and trace element concentrations are not likely to occur in rocks which have experienced both high and low temperature hydrothermal alteration. Sr can evidently be partitioned strongly into feldspar at low temperatures such that the Sr concentrations of whole-rock samples

are significantly affected. On the other hand,  $^{18}\text{O}$  enrichments or depletions at low temperatures are confined to volumetrically minor portions of grains and the effects on whole-rock  $\delta^{18}\text{O}$  values are likely to be small.

The effects of hydrothermal alteration on Sr isotope ages are systematic, not random. The mismatch of scales of Sr transport and isotopic equilibration demonstrates a potentially important effect of subsolidus alteration: addition of radiogenic Sr forms correlations between Rb/Sr ratios and  $^{87}\text{Sr}/^{86}\text{Sr}$  ratios and the present-day Rb—Sr relations of whole-rock samples are not age significant. The theoretical explanation of such “age shifts” is presented elsewhere (Lutz & Srogi, 1986) but, in general, age shifts are *expected* from subsolidus Sr alteration. Significant shifts may occur even when the amounts of Sr added are small and are uncorrelated with the original Sr and Rb concentrations. A consequence of inaccurate dating of rocks is that petrogenetic interpretations based on calculated initial  $^{87}\text{Sr}/^{86}\text{Sr}$  may be in error. Any isotopic variations which may have originally existed can be obscured or distorted by subsolidus alteration.

Analyses of minerals from the Abu Khruq syenites were crucial to understanding the nature of the alteration process and its effects. The rims of minerals, or the edges of microfractures within them, are the primary sites at which interactions between rock and fluid take place. Depending on the history of the hydrothermal event, mineral-scale heterogeneities in trace element concentrations and isotopic compositions may develop within minerals grains. The chemical variations in, and scale of, such heterogeneities are essential to understanding the chemical variations in whole-rock samples. This is especially true for minerals such as feldspar which may contain substantial portions of the whole-rock Sr budget.

The more highly altered rims of grains may be unintentionally removed from mineral separates because they tend to be concentrated in particles which are compound. Careful control of the mineral separation procedure is required to detect intramineral heterogeneities, especially since a stain or other physical feature may not be characteristic of grain rims.

A consequence of the decoupling of trace element and Sr isotopic alteration of rocks from oxygen isotopic and mineralogic alteration is that there is no effective way to detect the chemical effects of hydrothermal alteration from whole-rock samples alone. The possibility of subsolidus chemical alteration should be considered whenever rocks show any evidence of hydrothermal interaction. As a first step, analysis of mineral separates must be done. Intramineral variations in trace element concentrations which cannot be explained by magmatic processes (e.g., high-Sr rims on alkali feldspars) are the most unambiguous evidence of hydrothermal interaction.

*Acknowledgments.* We are grateful to Irving Friedman and Jim Gleason of the USGS, Denver, for use of analytical facilities and help in performing O isotopic analyses. We also gratefully acknowledge our collaborators with the Geological Survey of Egypt, particularly M.F. El Ramly and A.A.A. Hussein.

Financial support was provided, in part, by grants from the National Science Foundation (EAR73-00195-A02 and EAR77-13634 to KAF) and the Smithsonian Foreign Currency Program (to HF). Manuscript preparation was supported by a grant from the Research Foundation of the University of Pennsylvania (to TML).

We are grateful to Robert Criss for a thorough review of the manuscript.

## References

- Brooks C, Hart SR, Wendt I (1972) Realistic use of two-error regression treatments as applied to Rb—Sr data. *Rev Geophys Space Phys* 10:551–577
- Cathelineau M (1987) U-Th-REE mobility during albitization and quartz dissolution in granitoids: evidence from south-east French Massif Central. *Bull Minéral* 110:249–259
- Clayton RN, Mayeda T (1963) The use of bromine pentafluoride in the extraction of oxygen from oxides and silicates for isotopic analysis. *Geochim Cosmochim Acta* 27:43–52
- Criss RE, Fleck RJ (1987) Petrogenesis, geochronology, and hydrothermal systems of the northern Idaho Batholith and adjacent areas based on  $^{18}\text{O}/^{16}\text{O}$ , D/H,  $^{87}\text{Sr}/^{86}\text{Sr}$ , K—Ar and  $^{40}\text{Ar}/^{39}\text{Ar}$  studies. *US Geol Surv Prof Pap* 1436:95–137
- Deer WA, Howie RA, Zussman JG (1966) An introduction to the rock-forming minerals. Longmans, Green and Co., London
- Dickin AP (1983) Hydrothermal fluid pathways at the contact of the Beinn an Dubhaich epigranite, Isle of Skye. *Scot J Geol* 19:235–242
- Dickin AP, Jones NW (1983) Relative elemental mobility during hydrothermal alteration of a basic sill, Isle of Skye, NW Scotland. *Contrib Mineral Petrol* 82:147–153
- Dickin AP, Exley RA, Smith BM (1980) Isotopic measurement of Sr and O exchange between meteoric-hydrothermal fluid and the Coire Uaigneich Granophyre, Isle of Skye, NW Scotland. *Earth Planet Sci Lett* 51:58–70
- El Ramly MF, Hussein AAA (1985) The ring complexes of the Eastern Desert of Egypt. *J Afr Earth Sci* 3:77–82
- El Ramly MF, Dereniuk NE, Budanov VI, Armanious LK, Hayek GG (1969a) A petrological study on the central part of the Gabal Abu Khruq ring complex. *Geol Survey Egypt Pap no. 51*
- El Ramly MF, Armanious LK, Budanov VI, Dereniuk NE (1969b) The three ring complexes of Gabal El Kahfa, Gabal Nigrub El Fogani, and Gabal El Naga. *Geol Surv Egypt Pap no. 52*
- El Ramly MF, Budanov VI, Hussein AAA (1971) The alkaline rocks of south-eastern Egypt. *Geol Surv Egypt Pap no. 53*
- El Ramly MF, Armanious LK, Hussein AAA (1979) The two ring complexes of Hadayib and Um Risha, South Eastern Desert. *Ann Geol Surv Egypt* 9:61–69
- Fleck RJ, Criss RE (1985) Strontium and oxygen isotopic variations in Mesozoic and Tertiary plutons of central Idaho. *Contrib Mineral Petrol* 90:291–308
- Johnston C, Black LP (1986) Rb—Sr systematics of the Coolgarra Batholith, North Queensland. *Aust J Earth Sci* 33:309–324
- Kendall M (1975) Rank correlation methods. Charles Griffin
- Lutz TM, Srogi L (1986) Biased isochron ages resulting from subsolidus isotope exchange: a theoretical model and results. *Chem Geol* 56:63–71
- McCulloch MT, Gregory RT, Wasserburg GJ, Taylor HP Jr (1981) Sm—Nd, Rb—Sr, and  $^{18}\text{O}/^{16}\text{O}$  isotopic systematics in an oceanic crustal section: evidence from the Samail ophiolite. *J Geophys Res* 86:2721–2735
- Neary CR, Gass IG, Cavanagh BJ (1976) Granitic association of northeastern Sudan. *Bull Geol Soc Am* 87:1501–1512
- Omar GI, Kohn BP, Lutz TM, Faul H (1987) The cooling history of Devonian to Cretaceous alkaline ring complexes in southeast Egypt as revealed by fission-track dating. *Earth Planet Sci Lett* 83:94–108
- Perfit MR, Brueckner H, Lawrence JR, Kay RW (1980) Trace element and isotopic variations in a zoned pluton and associated volcanic rocks, Unalaska Island, Alaska: a model for fractionation in the Aleutian calcalkaline suite. *Contrib Mineral Petrol* 73:69–87
- Schleicher H, Lippolt HJ, Raczek I (1983) Rb—Sr systematics of Permian volcanites in the Schwarzwald (SW-Germany). Part II: Age of eruption and the mechanism of Rb—Sr whole rock age distortions. *Contrib Mineral Petrol* 84:281–291

- Serencsits C McC, Faul H, Foland KA, El Ramly MF, Hussein AA (1979) Alkaline ring complexes in Egypt: their ages and relationship to tectonic development of the Red Sea. *Ann Geol Surv Egypt* 9:102–116
- Serencsits C McC, Faul H, Foland KA, Hussein AA, Lutz TM (1981) Alkaline ring complexes in Egypt: their ages and relationship in time. *J Geophys Res* 86:3009–3013
- Spooner ETC, Chapman HJ, Smewing JD (1977) Strontium isotopic contamination and oxidation during ocean floor hydrothermal metamorphism of the ophiolitic rocks of the Troodos Massif, Cyprus. *Geochim Cosmochim Acta* 41:873–890
- Steiger RH, Jäger E (1977) Subcommittee on geochronology: convention on the use of decay constants in geo- and cosmochronology. *Earth Planet Sci Lett* 36:359–362
- Stuckless JS, Nkomo IT, Doe BR (1981) U–Th–Pb systematics in hydrothermally altered granites from the Granite Mountains, Wyoming. *Geochim Cosmochim Acta* 45:635–645
- Taylor HP Jr (1974) The application of oxygen and hydrogen isotope studies to problems of hydrothermal alteration and ore deposition. *Econ Geol* 69:843–883
- Taylor HP Jr (1977) Water/rock interactions and the origin of H<sub>2</sub>O in granitic batholiths. *J Geol Soc London* 133:509–558
- Taylor HP Jr (1978) Oxygen and hydrogen isotope studies of plutonic granitic rocks. *Earth Planet Sci Lett* 38:177–210
- Vail JR (1976) Location and geochronology of igneous ring-complexes and related rocks in north-east Africa. *Geol Jahrb* 20:97–114
- Walsh JN, Beckinsale RD, Skelhorn RR, Thorpe RS (1979) Geochemistry and petrogenesis of Tertiary granitic rocks from the Island of Mull, northwest Scotland. *Contrib Mineral Petrol* 71:99–116
- York D (1969) Least squares fitting of a straight line with correlated errors. *Earth Planet Sci Lett* 5:320–324

Received March 12, 1987 / Accepted October 27, 1987

Editorial responsibility: I.S.E. Carmichael